UNIFICATION OF SIGNAL MODELS FOR SOQPSK

Erik Perrins
Department of Electrical Engineering and Computer Science
University of Kansas
Lawrence, KS 66045 USA
esp@ieee.org

Michael Rice
Department of Electrical and Computer Engineering
Brigham Young University
Provo, UT 84602 USA
mdr@byu.edu

ABSTRACT

This paper begins by summarizing a recent advancement in the way that shaped offset quadrature phase shift keying (SOQPSK) waveforms can be viewed. This new viewpoint succeeds in eliminating the need for SOQPSK to be thought of as a "special" kind of correlated, ternary continuous phase modulation (CPM). Instead, SOQPSK can be viewed as an ordinary, binary CPM. We provide all of the details necessary to achieve a complete unification of SOQPSK models at the waveform level, at the bit sequence level, and in terms of waveform initialization. With this information, SOQPSK users can easily mix and match SOQPSK models at the transmitter and receiver in order to make use of the advantages of each model.

INTRODUCTION

Over the past few decades, various models for shaped offset quadrature phase shift keying (SOQPSK) have been developed. The original motivation for SOQPSK was to yield a waveform with continuous phase and constant envelope that had OQPSK-like characteristics. Out of this was developed special continuous phase modulation (CPM) model for SOQPSK [1, 2]. However, unlike ordinary CPM waveforms, this model describes SOQPSK as a CPM waveform that is driven by a correlated ternary data sequence. This model has since been used to describe the waveform itself in standards, i.e. [3, 4], and thus is always used in transmitter implementations that generate SOQPSK waveforms. At the receiver, however, one has the flexibility of using the special CPM detection model or a simple symbol-by-symbol OQPSK-type detection model, e.g. [5].

Recently, Othman et al. [6] developed a new model for SOQPSK that completely eliminates the need for the correlated ternary CPM model for SOQPSK. They showed that SOQPSK can be viewed as an ordinary binary CPM. Because of the need for mixing and matching models

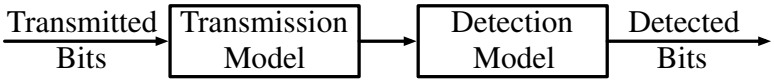

Figure 1: Transmission and Detection models for SOQPSK.

at transmitters and receivers, the introduction of this new model creates the need for a unified presentation of all SOQPSK models and a detailed explanation of how to switch from one model to another. The aim of this paper is to fill this need. In fact, our paper demonstrates that the term "SOQPSK-TG," along with its extensive list of attendant definitions, could be completely removed from IRIG-106 and replaced with the term "binary CPM with $h = 1/2$ and an $L = 9$ custom frequency pulse," with no additional definitions needed. Such a simplifying change could be made with no tangible difference to the signal itself.

We begin by presenting the various signal models for SOQPSK. This presentation includes a detailed description of the different data sequences used in each model, and how to switch between them. We also show how the IRIG-106 differential encoder figures into the situation. Our consideration includes details on how these different sequences and waveforms can be initialized to preserve their equivalence. We then give two detailed use cases that show how all of these details can be properly applied.

CLASSICAL MODEL FOR SOQPSK AS A SPECIAL CPM

We consider the classical SOQPSK signal model with complex envelope [7]

$$s_{\mathrm{s}}(t;\mathbf{a}) = \sqrt{\frac{E_b}{T_b}}\exp\left\{j\big(\phi_{\mathrm{s}}(t;\mathbf{a}) + \theta_{\mathrm{s}}\big)\right\} \tag{1}$$

where E_b is the energy per information bit and T_b is the bit duration. The value of the static phase offset θ_{s} is defined later. The time-varying phase term in (1) is a pulse train of the form

$$\phi_{\mathrm{s}}(t;\mathbf{a}) = 2\pi h\sum_i \alpha_i q_{\mathrm{s}}(t - iT_b) \tag{2}$$

where $h = 1/2$ is the modulation index. The *phase response* $q_{\mathrm{s}}(t)$ is usually thought of as the time-integral of a *frequency pulse* $g_{\mathrm{s}}(t)$ with area 1/2 and duration LT_b. The subscript "S" signifies variables that belong to the classical SOQPSK model. There are multiple standardized versions of SOQPSK, which differ from each other by the shape and duration of their respective frequency pulses, $g_{\mathrm{s}}(t)$. In this paper we focus on SOQPSK-MIL [3], which uses a full-response ($L = 1$) rectangular frequency pulse (1REC), and SOQPSK-TG [4], which uses a partial-response (meaning $L_{\mathrm{s}} > 1$ and in this case $L_{\mathrm{s}} = 8$) custom pulse shape defined in [8, Eq. (5)] and plotted in [8, Fig. 1].

The transmitted ternary symbols $\boldsymbol{\alpha} = \{\alpha_i\}$ are derived from a binary antipodal input sequence $\mathbf{a} = \{a_i\}$ by a *precoding* operation [1]

$$\alpha_i = \frac{1}{2}(-1)^{i+1}a_{i-1}(a_i - a_{i-2}), \qquad a_i \in \{\pm 1\}, \qquad \alpha_i \in \{-1, 0, +1\}, \tag{3}$$

Table 1: Key Parameters for the Different SOQPSK Signal Models.

Name	Native Sequence	Derived Sequences	Initialization
Classical/Special CPM	$\mathbf{a} = \{a_i\}$	$\boldsymbol{\alpha} = \{\alpha_i\}$ [Eq. (3)] and $\boldsymbol{\gamma} = \{\gamma_i\}$ [Eq. (6)]	$a_{-2} = +1$, $a_{-1} = -1$, $\theta_{\mathrm{s}} = -\pi/4$ (-45°)
New/Ordinary CPM	$\boldsymbol{\gamma} = \{\gamma_i\}$	$\mathbf{a} = \{a_i\}$ [Eq. (17)] or $\mathbf{b}_0 = \{b_{0,i}\}$ [Eqs. (11) and (12)]	$\gamma_{-1} = -1$
PAM/OQPSK	$\mathbf{a} = \{a_i\}$ or $\mathbf{b}_0 = \{b_{0,i}\}$	$\boldsymbol{\gamma} = \{\gamma_i\}$ [Eq. (6)]	$a_{-2} = +1$, $a_{-1} = -1$, or $b_{0,-2} = +1$, $b_{0,-1} = -j$

The precoder constrains the symbol sequence such that not every possible ternary symbol pattern is a valid SOQPSK data pattern. For example, the ternary symbol sequences $\ldots, 0, +1, -1, 0, \ldots$ and $\ldots, +1, 0, +1, \ldots$ are not possible due to the precoder. These constraints can be summarized as [1]:

1. While α_i is viewed as being *ternary*, in any given bit interval α_i is actually drawn from one of two *binary* alphabets, $\{0, +1\}$ or $\{0, -1\}$.
2. When $\alpha_i = 0$, the binary alphabet for α_{i+1} switches from the one used for α_i, when $\alpha_i \neq 0$ the binary alphabet for α_{i+1} does not change.
3. A value of $\alpha_i = +1$ cannot be followed by $\alpha_{i+1} = -1$, and vice versa (this is implied by the previous constraint).

We use the notation $s_{\mathrm{s}}(t; \mathbf{a})$ to underscore the fact that $\mathbf{a}$ is driving the signal. The reason for this non-obvious precoding operation is that (3) orients the phase of the SOQPSK signal in (1) such that it behaves like the phase of an OQPSK signal that is driven by the i.i.d. bit sequence $\mathbf{a}$. In fact, $\mathbf{a}$ can be recovered directly from the received signal, with no additional steps, by a suboptimal symbol-by-symbol OQPSK-type detector [9, 10]. Because of this, $\mathbf{a} = \{a_i\}$ is viewed as the "native" (or "original") sequence for this signal model. Table 1 contains a row that summarizes key parameters for the classical model for SOQPSK, some of which are explained in later sections.

NEW MODEL FOR SOQPSK AS AN ORDINARY CPM

In a recent paper by Othman et al. [6], the authors reformulated the precoder in (3) as

$$\alpha_i = \frac{1}{2}\left[(-1)^{i+1} a_i a_{i-1} + (-1)^i a_{i-1} a_{i-2}\right] \tag{4}$$

$$= \frac{1}{2}\left[\gamma_i + \gamma_{i-1}\right] \tag{5}$$

where

$$\gamma_i = (-1)^{i+1} a_i a_{i-1}, \qquad \gamma_i, a_i \in \{\pm 1\}. \tag{6}$$

By inserting (5) into (2), they showed that the signal's phase can be written as

$$\phi_{\mathrm{c}}(t; \boldsymbol{\gamma}) = 2\pi h \sum_i \gamma_i q_{\mathrm{c}}(t - iT_b) \tag{7}$$

where a different phase response is obtained as [6, Eq. (15)]

$$q_{\mathrm{C}}(t) = \frac{1}{2}\left[q_{\mathrm{S}}(t) + q_{\mathrm{S}}(t - T_b)\right], \tag{8}$$

This, in turn, implies the definition of a new frequency pulse $f_{\mathrm{C}}(t)$ that has a duration one bit time longer than $f_{\mathrm{S}}(t)$, i.e. $L_{\mathrm{C}} = L_{\mathrm{S}} + 1$. We use a subscript "C" to signify variables that belong to this new CPM model. Summarized succinctly, a ternary model for SQOSPK with $q_{\mathrm{S}}(t)$ and L_{S} is identical *at the waveform level* with an ordinary binary antipodal ($M = 2$) CPM model with $q_{\mathrm{C}}(t)$ and L_{C}.

Thus, the ordinary CPM scheme better known as $M = 2$, $h = 1/2$, 2REC is equivalent to the SOQPSK-MIL waveform. The bandwidth efficiency of SOQPSK-MIL over MSK was previously attributed to the correlation in the ternary data symbols. Now, this bandwidth efficiency is revealed to be the result of lengthening the frequency pulse from 1REC to 2REC, which is entirely consistent with standard CPM behavior e.g. [7]. Likewise, the SOQPSK-TG waveform gains its spectral efficiency by using an even longer and smoother frequency pulse than originally conceived, with a duration of $L_{\mathrm{C}} = 9$ bit intervals.

What (7) describes is an ordinary binary antipodal CPM whose native sequence is $\boldsymbol{\gamma}$. The complex baseband representation of this signal is

$$s_{\mathrm{C}}(t; \boldsymbol{\gamma}) = \sqrt{\frac{E_b}{T_b}} \exp\left\{j\phi_{\mathrm{C}}(t; \boldsymbol{\gamma})\right\} \tag{9}$$

Table 1 contains a row that summarizes key parameters for the new CPM model for SOQPSK.

OQPSK MODEL FOR SOQPSK

Because of this new binary CPM model, SOQPSK signals are nothing more than regular MSK-type CPMs, i.e. CPMs that have $M = 2$ and $h = 1/2$. A popular and important way of handling such CPMs is the PAM representation of CPM, originally developed by Laurent in [11]. This representation offers a direct path for an OQPSK model for MSK-type CPMs. A binary CPM signal can be exactly represented as

$$s_{\mathrm{C}}(t; \boldsymbol{\gamma}) = \sqrt{\frac{E_b}{T_b}} \sum_{k=0}^{N-1} \sum_{i} b_{k,i}\, g_k(t - iT_b), \qquad N = 2^{L_{\mathrm{C}}-1} \tag{10}$$

where the *pseudo-symbols* $\{b_{k,i}\}$ and signal pulses $\{g_k(t)\}$ are found via the formulas in [11]. For SOQPSK-MIL, the exact representation consists of $N = 2$ signal pulses plotted in Figure 2 (a). For SOQPSK-TG, the exact representation consists of $N = 256$ signal pulses, the first four of which are plotted in Figure 2 (b). As these plots show, the first signal pulse—called the *main pulse* by Laurent and the *principal pulse* by others, e.g. [12]— carries nearly all the signal energy.

For MSK-type CPMs, the main pulse also carries all of the information [11], and its pseudo-symbols can be formulated by defining a *phase state index*

$$I_i = \left[\sum_{l=-\infty}^{i} \gamma_l\right]_{\text{mod } 4} \tag{11}$$

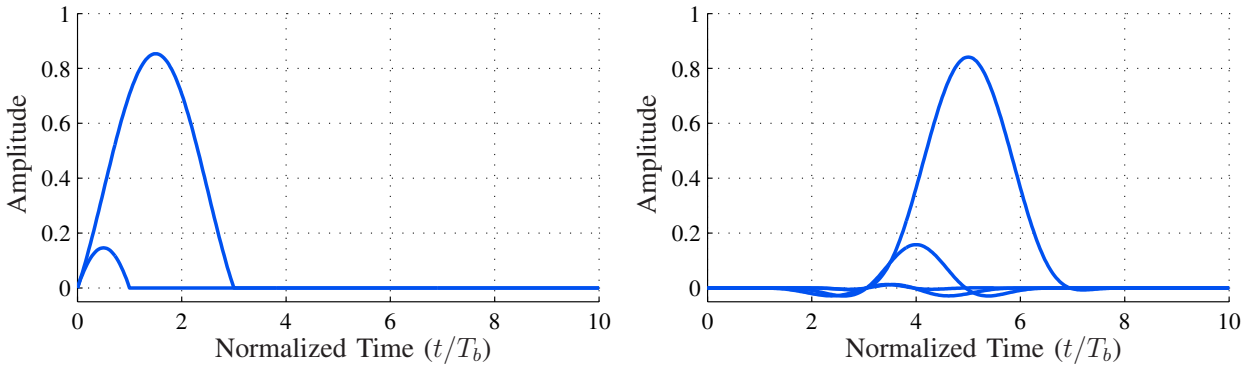

(a) (b)

Figure 2: (a) The two signal pulses that result in the exact PAM representation of SOQPSK-MIL. (b) The first four signal pulses in the approximate PAM representation of SOQPSK-TG.

which then appears in the exponent of the pseudo-symbol

$$b_{0,i} = e^{j\frac{\pi}{2}I_i} = j^{I_i}, \qquad b_{0,i} \in \{\pm 1, \pm j\} \tag{12}$$

where the mod 4 operation in (11) and the value $\pi/2$ in (12) stem from the modulation index being $h = 1/2$ [7].

Using the main pulse alone, the OQPSK approximation of the SOQPSK signal is given by

$$s_{\mathrm{O}}(t;\mathbf{a}) = \sqrt{\frac{E_b}{T_b}} \sum_i b_{0,i}\, g_0(t - iT_b) \tag{13a}$$

$$= \sqrt{\frac{E_b}{T_b}} \sum_{i \text{ even}} a_i\, g_0(t - iT_b) + \sqrt{\frac{E_b}{T_b}} \sum_{i \text{ odd}} j a_i\, g_0(t - iT_b) \tag{13b}$$

where the sequence $\mathbf{a}$ in (13b) is the same as the one in (1) because of the arguments presented in [2]. Thus, we have

$$a_i = \begin{cases} \mathrm{Re}\,\{b_{0,i}\} & i \text{ is even} \\ \mathrm{Im}\,\{b_{0,i}\} & i \text{ is odd} \end{cases} \tag{14}$$

We further manipulate this expression, assuming i is even, as

$$a_i = \mathrm{Re}\left\{j^{I_i}\right\} = \mathrm{Re}\left\{j^{\gamma_i} j^{I_{i-1}}\right\} \tag{15}$$

Because $\gamma_i \in \{\pm 1\}$, then $j^{\gamma_i} \in \{\pm j\}$, where the sign follows the sign of γ_i. Consequently

$$a_i = \mathrm{Re}\left\{j^{\gamma_i} j^{I_{i-1}}\right\} = -\gamma_i \mathrm{Im}\{j^{I_{i-1}}\} = -\gamma_i a_{i-1} \tag{16}$$

Repeating the above steps when i is odd yields the inverse relationship to (6) as

$$a_i = (-1)^{i+1} \gamma_i a_{i-1} \tag{17}$$

This provides the final link between $\mathbf{a}$ and $\boldsymbol{\gamma}$. Also, as (13) and (14) indicate, the pseudo-symbols $\{b_{0,i}\}$ are simply the binary antipodal sequence $\mathbf{a}$ expressed in an alternating inphase/quadrature format. Table 1 contains a row that summarizes key parameters for the PAM/OQPSK model for SOQPSK.

IRIG-106 DIFFERENTIAL ENCODING SCHEME FOR SOQPSK

The IRIG-106 standard specifies a differential encoding scheme for SOQPSK. We now show how this differential encoding scheme is equivalent to the $\boldsymbol{\gamma} \leftrightarrow \mathbf{a}$ relationship above. The differential encoder and decoder are specified in [4, Appendix M] using logical (Boolean) variables and notation; however, for our present purpose, we must convert these variables to an antipodal format. We denote a logical variable with a $'$ mark, i.e. $\gamma' \in \{0, 1\}$, and its antipodal counterpart without such a mark, i.e. $\gamma \in \{\pm 1\}$. There are two possible mappings between logical and antipodal variables. Although it is less common, the mapping

$$\gamma = 1 - 2\gamma' \tag{18}$$

yields the equivalence we seek to demonstrate.

The differential encoder has input sequence $\boldsymbol{\gamma}' = \{\gamma_i'\}$ and output sequence $\mathbf{a}' = \{a_i'\}$. The relationship between these sequences is defined as [4, Appendix M]

$$a_i' = \begin{cases} \gamma_i' \oplus \bar{a}_{i-1}' & i \text{ is even} \\ \gamma_i' \oplus a_{i-1}' & i \text{ is odd} \end{cases} \tag{19}$$

where even-indexed bits correspond to *inphase* (I) bits and odd-indexed bits correspond to *quadrature* (Q) bits, $\bar{a}'$ is the logical (Boolean) complement of a', and $\oplus$ is the Boolean XOR operation. The inverse of this relationship, i.e. the differential decoder, is defined as [4, Appendix M]

$$\gamma_i' = \begin{cases} a_i' \oplus \bar{a}_{i-1}' & i \text{ is even} \\ a_i' \oplus a_{i-1}' & i \text{ is odd} \end{cases} \tag{20}$$

The antipodal equivalents of (19) and (20) are, respectively,

$$a_i = (-1)^{i+1}\gamma_i a_{i-1} = \begin{cases} -\gamma_i a_{i-1} & i \text{ is even} \\ \gamma_i a_{i-1} & i \text{ is odd} \end{cases} \tag{21}$$

and

$$\gamma_i = (-1)^{i+1} a_i a_{i-1} = \begin{cases} -a_i a_{i-1} & i \text{ is even} \\ a_i a_{i-1} & i \text{ is odd} \end{cases} \tag{22}$$

For example, when i is even in (19), the operation of the differential encoder can be described as "the value of a_i' is the opposite of a_{i-1}' when $\gamma_i' = 0$." When i is even for the antipodal version in (21), its operation can be described as "the value of a_i is the opposite of a_{i-1} when $\gamma_i = +1$." These two statements are equivalent for the logical-to-antipodal mapping of $0 \longrightarrow +1$ in (18). Additional statements such as these verify the expressions above.

As (21) and (22) demonstrate, the $\boldsymbol{\gamma} \leftrightarrow \mathbf{a}$ relationship in the IRIG-106 differential encoder is identical to the relationship shown earlier in (6) and (17).

INITIALIZATION SCHEME

Table 1 defines initial values that must now be explained. The OQPSK model assumes in (14) that bits transmitted during even-indexed bit times are I bits, and bits transmitted during odd-indexed bit times are Q bits. We define n as the current bit index, where $nT_b \leq t < (n+1)T_b$. An initial value of $\gamma_{-1} = -1$, with all prior values initialized as

$$\gamma_i = 0, \qquad i \leq -2 \tag{23}$$

introduces a $\pi/2$ ($-90°$) phase value in (12) that results in $b_{0,-1} = ja_{-1} = -j$. This also means that $b_{0,-2} = a_{-2} = +1$. With this initialization (or an equivalent one based on $\gamma_{-1} = +1$), the transmission will commence with an I bit at $n = 0$, i.e. $b_{0,0} = a_0 \in \pm 1$.

However, the work of Othman et al. [6] exposes the necessity for one more initialization. In (5), the phase input for the first transmitted bit γ_0 is divided into halves, which are delivered in the consecutive bit intervals belonging to $n = 0$ and $n = 1$. This consecutive input behavior is also the case for all subsequent γ_i, i.e. $\{\gamma_i\}_{i \geq 0}$. However, this repetition does not happen for the initial symbol γ_{-1}, where only one half of its value is delivered when $n = 0$ and the other half never at all. As such, there is a discrepancy between the classical model for SOQPSK and the other two signal models of one "half-symbol" that cannot be resolved by initial symbols alone. We resolve this with a static phase offset of $\theta_s = -\pi/4$ ($-45°$) in the SOQPSK signal in (1). The initialization values in Table 1 are now fully explained.

The correctness of these initialization values—in particular $\theta_s = -\pi/4$—is verified by the sample signals plotted in Figures 3 and 4 for SOQPSK-MIL and SOQPSK-TG, respectively. In the case of Figure 3 (SOQPSK-MIL), there is no observable difference between the classical SOQPSK model and the new CPM model. The slight difference between the OQPSK/PAM model and the other two models is due to the fact that only the main PAM pulse from Figure 2 (a) is used to generate the example signal.

In the case of Figure 4 (SOQPSK-TG), the OQPSK/PAM model and the other two models differ again due to the main pulse approximation from Figure 2 (b). However, there is also an initial transient difference between the classical SOQPSK model and the new CPM model. This transient is due to the fact that the $L_c = 9$ CPM phase response is initialized mostly with zero-valued γ_i symbols, as specified in (23). A value of zero does not belong to the binary antipodal alphabet in the strict sense, but it does belong to the ternary alphabet. Thus, there is a transient mismatch between the $\boldsymbol{\gamma}$ and $\mathbf{a}$ sequences. Such a sequence of ternary zeroes could be generated by $(-1, +1)$ pairs for the γ_i symbols. Pre-pending three such pairs (all the way back to $\gamma_{-7} = -1$ and $\gamma_{-6} = +1$) will eliminate this transient discrepancy altogether yet will still preserve the expected ordering of I/Q bits. In the case of SOQPSK-MIL, the $L_c = 2$ CPM phase response already has a valid binary antipodal symbol for its initial value and such pre-pending is not necessary. We have opted for a "one-size-fits-all" initialization scheme in Table 1, with the understanding that users who specialize only in SOQPSK-TG may wish to adopt the additional initialization values mentioned above.

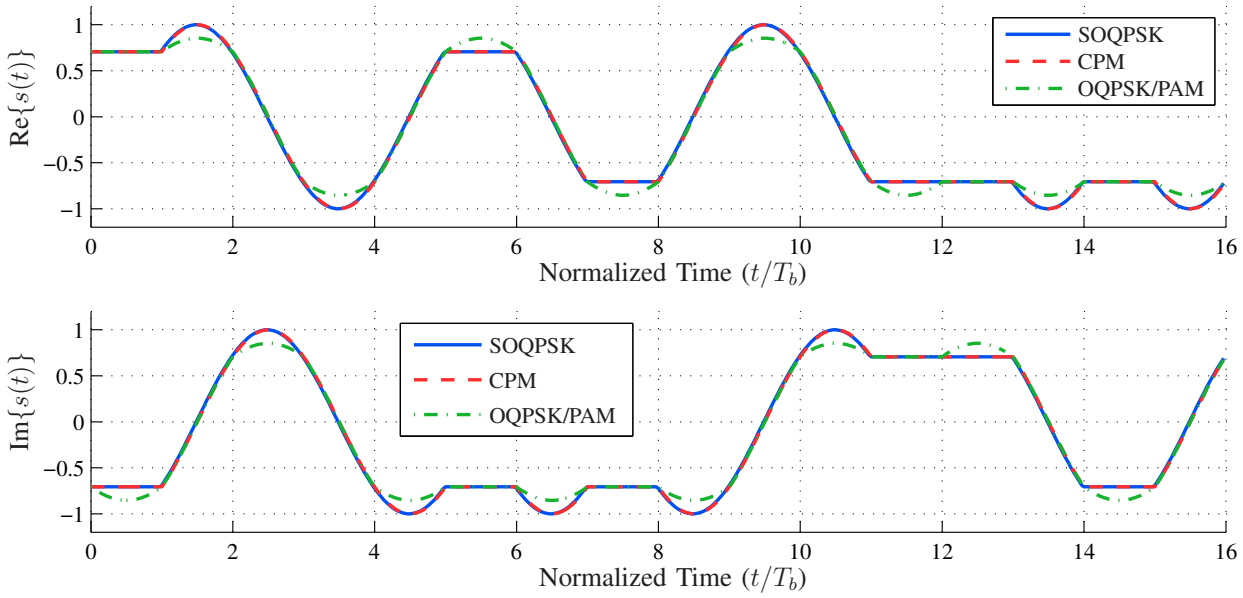

Figure 3: Sample signals for the three signal models for SOQPSK-MIL (the real part is shown in the upper plot and the imaginary part is shown in the lower plot). There is no observable difference between the classical SOQPSK model and the new CPM model. The OQPSK/PAM model shows slight differences because only the main PAM pulse in Figure 2 (a) is used.

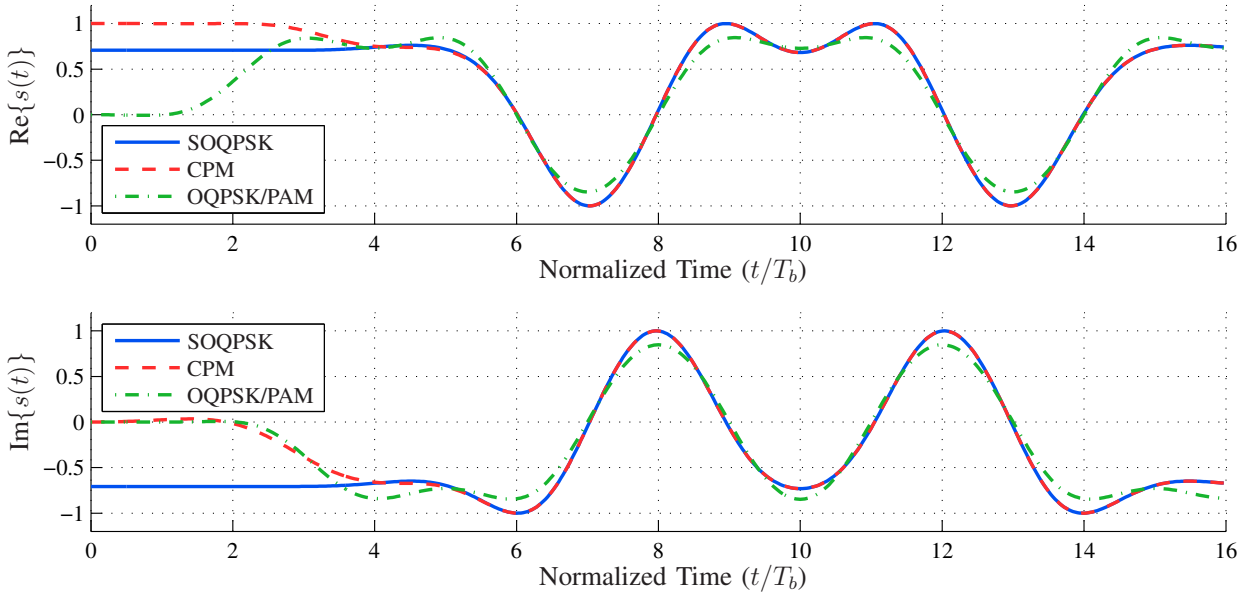

Figure 4: Sample signals for the three signal models for SOQPSK-TG (the real part is shown in the upper plot and the imaginary part is shown in the lower plot). There is an initial transient difference between the classical SOQPSK model and the new CPM model that could be resolved with a different initialization scheme. The OQPSK/PAM model shows slight differences because only the main PAM pulse in Figure 2 (b) is used.

USE CASE #1: A SYSTEM WHERE $\boldsymbol{\gamma}$ IS THE INFORMATION SEQUENCE: A.K.A. IRIG-106 DIFFERENTIAL ENCODED SOQPSK

We now explore detailed use cases based on Figure 1. We first consider an arrangement where $\boldsymbol{\gamma}$ serves as the information sequence and the transmitter implements the ordinary CPM model. If we pair this transmitter with its matching CPM detection model, then the entire end-to-end system is well understood [7]. As described in [7], the detector uses a Viterbi algorithm (VA) implementation with a $2pM^{L_c-1}$ state trellis, where $p = 2$ is the denominator of $h = 1/2 = 1/p$; this yields in an 8-state trellis for SOQPSK-MIL and a 1024-state trellis for SOQPSK-TG. Such a trellis tolerates phase shifts of $2\pi/(2p) = \pi/2$ without any negative effects and requires timing to be resolved on a single bit basis only. Using the "tilted phase" model [13], the trellis size can be reduced to pM^{L_c-1} states (4 states for SOQPSK-MIL and 512 states for SOQPSK-TG); however, the tilted-phase trellis is tolerant of $2\pi/p = \pi$ phase shifts and it must resolve symbol timing of even and odd bit intervals. Another consequence of tilted phase is that a timing shift of a single bit interval and a phase shift of $\pm\pi/2$ (i.e. an even/odd–I/Q swap) are indistinguishable from each other at the receiver.

For all SOQPSK versions and trellis types, the minimum and second minimum squared Euclidean distances, respectively, belong to sequence pairs that satisfy [8]

$$\hat{\boldsymbol{\gamma}} - \boldsymbol{\gamma} = \pm\{\ldots, 0, +2, -2, 0, \ldots\} \tag{24a}$$

and

$$\hat{\boldsymbol{\gamma}} - \boldsymbol{\gamma} = \pm\{\ldots, 0, +2, +2, 0, \ldots\} \tag{24b}$$

We note that these error events result in pairs of bit errors. We also note the above insensitivity to certain phase and even/odd–I/Q shifts, and in fact, we have shown the equivalence between the $\boldsymbol{\gamma} \leftrightarrow \mathbf{a}$ relationship and the IRIG-106 differential encoder. The IRIG-106 standard specifies the following sequence of three steps needed to generate a SOQPSK signal:

$$\boldsymbol{\gamma} \longrightarrow \mathbf{a} \longrightarrow \boldsymbol{\alpha} \longrightarrow s_{\mathrm{s}}(t; \mathbf{a}) \tag{25}$$

Based on our efforts above, the following single step results in the same signal:

$$\boldsymbol{\gamma} \longrightarrow s_{\mathrm{c}}(t; \boldsymbol{\gamma}) \tag{26}$$

as verified by Figures 3 and 4.

A variation of this use case is to pair the ordinary CPM transmitter with the classical SOQPSK detector or an OQPSK detector. Here, the sequence initially detected by these models is their native one, $\hat{\mathbf{a}}$, which according to Table 1 can be converted to the desired information sequence $\hat{\boldsymbol{\gamma}}$ by feeding it through (6), which is equivalent to the IRIG-106 differential decoder in (20) and (22) when the proper antipodal-to-logical conversion is used.

USE CASE #2: A SYSTEM WHERE $\mathbf{a}$ IS THE INFORMATION SEQUENCE

The other arrangement of Figure 1 we explore is where the information sequence is $\mathbf{a}$. There has already been a thorough investigation of classical SOQPSK transmitters paired with their matching

detectors, e.g. [8, 14]. Therefore, we consider a different configuration where an ordinary CPM transmitter is paired with its matching detector. Because $\boldsymbol{\gamma}$ is the expected input for the ordinary CPM transmission model, we pass $\mathbf{a}$ through (6) to obtain $\boldsymbol{\gamma}$ at the transmitter. At the receiver, the ordinary CPM detector initially detects its native sequence, $\hat{\boldsymbol{\gamma}}$, which according to Table 1 can be converted to the desired information sequence $\hat{\mathbf{a}}$ by feeding it through (17). Although the difference sequences $\hat{\boldsymbol{\gamma}}$ in (24) contain *pairs* of errors, when subjected to the mod-4-accumulate operation in (11), the second error either cancels with the first, as in (24a), or sums to 4, as in (24b), resulting in an $\hat{\mathbf{a}}$ sequence with a single bit error. This demonstrates how an end-to-end CPM-type transmission can occur without differential encoding, i.e. with error events consisting of single-bit errors (as was done in [15]). Such a configuration without differential encoding is needed, for example, when SOQPSK is paired with an LDPC code [16, 4].

A variation of this use case is to pair the ordinary CPM transmitter with an OQPSK detector. Eq. (6) is again used to obtain $\boldsymbol{\gamma}$ at the transmitter. At the receiver, the OQPSK detector yields its native sequence, $\hat{\mathbf{a}}$, without the need for any additional processing.

CONCLUSION

The above use cases have drawn out the fact that enhancements for SOQPSK and CPM have unfolded on separate but parallel tracks, e.g. both have had their trellis size reduced by a factor of two with an accompanying impact on the synchronization behavior of the receiver, both have been used with and without differential encoding, etc. Prior to the work of Othman et al. in [6], there was no way to connect or unify these developments. Now that this unification has been established, these examples demonstrate that the classical SOQPSK model as special CPM is entirely redundant and can be discarded without consequence. In other words, SOQPSK is fully encompassed by an ordinary CPM model.

Establishing the equivalence of the waveforms is one important step. The other necessary detail we addressed is to establish the equivalence between the binary sequences used to drive the different waveform models. A related task is the proper initialization of these sequences and waveforms. The information in Table 1 provides this additional unification.

REFERENCES

[1] M. Simon, *Bandwidth-Efficient Digital Modulation With Application to Deep-Space Communication*. New York: Wiley, 2003.

[2] M. Simon and L. Li, (2003, Aug.), "A cross-correlated trellis-coded quadrature modulation representation of MIL-STD shaped offset quadrature phase-shift keying," *Interplan. Network Prog. Rep.*, vol. [Online]. Available: http://ipnpr.jpl.nasa.gov/tmo/progress_report/42-154/154J.pdf.

[3] D. I. S. Agency, "Department of Defense interface standard, interoperability standard for single-access 5-kHz and 25-kHz UHF satellite communications channels." Tech. Rep. MIL-STD-188-181B, Department of Defense, Mar. 1999.

[4] Range Commanders Council Telemetry Group, Range Commanders Council, White Sands Missile Range, New Mexico, *IRIG Standard 106-17: Telemetry Standards*, 2017. (Available on-line at http://www.wsmr.army.mil/RCCsite/Pages/Publications.aspx).

[5] M. Geoghegan, "Optimal linear detection of SOQPSK," in *Proc. Int. Telemetering Conf.*, Oct. 2002.

[6] R. Othman, A. Skrzypczak, and Y. Louët, "PAM decomposition of ternary CPM with duobinary encoding," *IEEE Trans. Commun.*, vol. 65, pp. 4274–4284, Oct. 2017.

[7] J. B. Anderson, T. Aulin, and C.-E. Sundberg, *Digital Phase Modulation*. New York: Plenum Press, 1986.

[8] E. Perrins and M. Rice, "Reduced-complexity approach to iterative detection of coded SOQPSK," *IEEE Trans. Commun.*, vol. 55, pp. 1354–1362, Jul. 2007.

[9] T. Hill, "A non-proprietary, constant envelope, variant of shaped offset QPSK (SOQPSK) for improved spectral containment and detection efficiency," in *Proc. IEEE Military Commun. Conf.*, Oct. 2000.

[10] M. J. Dapper and T. J. Hill, "SBPSK: A robust bandwidth-efficient modulation for hard-limited channels," in *Proc. IEEE Military Commun. Conf.*, Oct. 1984.

[11] P. A. Laurent, "Exact and approximate construction of digital phase modulations by superposition of amplitude modulated pulses (AMP)," *IEEE Trans. Commun.*, vol. 34, pp. 150–160, Feb. 1986.

[12] U. Mengali and M. Morelli, "Decomposition of M-ary CPM signals into PAM waveforms," *IEEE Trans. Inform. Theory*, vol. 41, pp. 1265–1275, Sep. 1995.

[13] B. E. Rimoldi, "A decomposition approach to CPM," *IEEE Trans. Inform. Theory*, vol. 34, pp. 260–270, Mar. 1988.

[14] L. Li and M. Simon, "Performance of coded OQPSK and MIL-STD SOQPSK with iterative decoding," *IEEE Trans. Commun.*, vol. 52, pp. 1890–1900, Nov. 2004.

[15] P. Galko and S. Pasupathy, "Linear receivers for correlatively coded MSK," *IEEE Trans. Commun.*, vol. 33, pp. 338–347, Apr. 1985.

[16] E. Perrins, "FEC systems for aeronautical telemetry," *IEEE Trans. Aerosp. Electron. Syst.*, vol. 49, pp. 2340–2352, Oct. 2013.